IEICE TRANSACTIONS

on Fundamentals of Electronics, Communications and Computer Sciences

DOI:10.1587/transfun.2024EAL2061

Publicized:2024/11/13

A PUBLICATION OF THE ENGINEERING SCIENCES SOCIETY

The Institute of Electronics, Information and Communication Engineers

Kikai-Shinko-Kaikan Bldg., 5-8, Shibakoen 3 chome, Minato-ku, TOKYO, 105-0011 JAPAN

LETTER

Multi-ship Formation Recognition for HFSWR in a Long Coherent Integration Time

Jiaqi Wang[†a)], ***Aijun Liu***[†b)], ***and*** **Changjun Yu**[†c)]

SUMMARY The deep learning method has been proven to be perfect in the field of multi-ship formation (MSF) recognition for high-frequency surface wave radar (HFSWR). However, the range-Doppler (RD) images of MSF are not always available in large quantities for training. And there is diversification in formation styles. In this paper, we propose a signal processing method for HFSWR formation recognition, which performs RD imaging through coherent accumulation and motion compensation. In the Doppler profile, the peaks are equal to sub-targets. The experiments based on actual RD background verify the feasibility and robustness of the proposed method.

key words: *high-frequency surface wave radar, motion compensate, formation recognition, robustness.*

1. Introduction

High-frequency surface wave radar (HFSWR) works in the 3-30MHz frequency band, which is able to monitor large areas of the sea surface in real time under all weather conditions [1,2]. The HFSWR can compensate for the blind spots in the line of sight detection and has wide applications in ship monitoring and maritime warning [3,4].

The existing research on target detection is chiefly conducted in the range-Doppler (RD) images [5], which are generated by 2D Fast-Fourier transform (FFT) processing of echo signals. Detection and distinction of dense ships in the field of HFSWR have limitation because of the spectral peak broadening and spectral peak adhesion caused by multiple targets aggregation. Many studies have focused on this. In the case of multiple targets in the same cell, Rohling H [6] used the optimal thresholding method to decide about the targets' presence. In [7], the adaptive constant false alarm rate (CFAR) threshold combined with pulse accumulation is introduced to improve resolution for many targets that are closely spaced in range, Doppler, and azimuth. Li et al. [8] analyzed the domain knowledge of spatial correlation and modified the existing constant false alarm detectors based on spatial information to improve the detection accuracy of dense targets.

The above researches in the field of HFSWR focus on the detection of irrelevant dense targets. Research on group targets with constraint principles, such as formation, is limited. The formation presents a certain spatial geometric shape, which is related to the relative position and motion of the sub-targets. In [9], the RD image model of multiple aircraft formation was established based on multipath effects. Based on this, the number of sub-targets in formation is accurately identified by the convolutional neural network (CNN) method in an ideal clutter background. In the previously published papers [10,11], we proposed a deep learning-based method for HFSWR multi-ship formation (MSF) recognition, and analyzed the radar measurement errors on MSF recognition accuracy. In practice, the RD images for MSF are not always available in large quantities for training. In some cases, the quantity information of sub-targets in the formation is more important than formation type information. In this paper, the signal processing based on the HFSWR formation model is introduced to distinguish formation. Firstly, the coherent accumulation is performed on the formation echo signal, and the Doppler resolution is improved by increasing coherent integration time (CIT). The overall motion compensation successfully eliminates the spectral peak broadening and spectral peak adhesion caused by multiple targets aggregation. Then, the RD processing is carried out, and the number of sub-targets is determined in the Doppler dimension through peak detection. Meanwhile, we analyze the radial velocity difference required for recognition and the radial velocity resolution provided by the radar system, and determine the CIT required for MSF recognition through experiments. The experimental process based on the actual RD background is provided, and the effectiveness of the proposed formation recognition method has been demonstrated. The Monte Carlo experiment verifies the robustness of the proposed method.

The rest of this paper is organized as follows. In Section Ⅱ, the MSF signal model and motion compensation method are introduced. In Section Ⅲ, the CIT and formation recognition results are discussed. In Section Ⅳ, a conclusion is drawn.

2. Ship Formation Recognition

In our previously established MSF model for HFSWR [10], the distance between sub-target p_i and the HFSWR station can be expressed as:

$$R_i = R(t) + r_i - l_i \cdot \triangle\theta \tag{1}$$

†The authors are with the College of Information Science and Engineering, Harbin Institute of Technology, Weihai 264209, China.
a) E-mail: 21B905018@stu.hit.edu.cn
b) E-mail:liuaijun@hit.edu.cn
c) E-mail:yuchangjun@hit.edu.cn

where $R(t)$ is the distance between the formation center and HFSWR station, r_i is the projected distance of the sub-target p_i relative to the formation center in the direction of radar line-of-sight, l_i is the projected distance of the sub-target p_i relative to the formation center perpendicular to the radar line-of-sight direction, and $\triangle\theta$ is the angle at which the formation center rotates relative to the HFSWR during CIT. The $R(t)$ and $\triangle\theta$ are related to the overall movement of the MSF, while r_i and l_i are related to the motion of the sub-targets relative to the formation center.

$$R(t) = R_0 + v_r \cdot t \tag{2}$$

where R_0 is the distance between the formation center and HFSWR station at the initial moment, and v_r is the radial velocity of the formation center relative to the HFSWR station.

Based on the consistent movement of the sub-targets, the compensation function for the MSF signal model is established and can be expressed as follows:

$$H(t) = \exp\left(-j\frac{4\pi}{c}\left(f_c R(t) + \frac{B}{T_c}R(t)t\right)\right) \tag{3}$$

where f_c, B, c and T_c represent the carrier frequency, system bandwidth, signal propagation speed and sweep period.

The uncompensated and compensated phase change of the sub-target p_i can be expressed as a combination of fast time t_f and slow time t_s:

$$\varphi_{p_i}' = \frac{2Br_i}{cT_c}t_f + \frac{2f_c r_i}{c} - \frac{v_{ri}}{c}t_s + \frac{2}{c}f_c R(t) + \frac{2B}{cT_c}R(t)\cdot t_s \tag{4}$$

$$\varphi_{p_i} = \frac{2Br_i}{cT_c}t_f + \frac{2f_c r_i}{c} - \frac{v_{ri}}{c}t_s \tag{5}$$

where v_{ri} is the radial velocity of the sub-target p_i, and $v_{ri} = l_i \cdot \triangle\theta / (t_f + t_s)$.

The fast time has a Fourier transform relationship with the radial projection distance r_i , and the slow time has a Fourier transform relationship with the radial velocity v_{ri} and v_r.The RD images are generated by performing 2D FFT along the fast time domain and slow time domain on the echo, respectively. Among them, the one-dimensional Doppler profile is obtained along the slow time domain.

3. Experiments

3.1 Resolution Performance Analysis

Table 1 HFSWR simulation parameters.

Parameter Name	Parameter symbol	Parameter Value
Carrier Frequency	f_c	6 MHz
Bandwidth	B	30 kHz
Sweep time	/	0.128 s
Pulse width	T_0	0.40 ms
Sampling Frequency	f_0	24 MHz

Table 2 MSF simulation parameters.

Parameter Name	Parameter symbol	Parameter Value
Distance between the formation center and HFSWR station	R_0	100 km
Azimuth angle of the formation center	θ_0	60°
Sailing speed	v_{ship}	8 m/s
Distance between formation center and sub-targets	d	2 km

The HFSWR system parameters are given in Table 1, and the MSF simulation parameters are given in Table 2.

The radial velocity is used to separate the sub-targets, of which resolution is related to CIT:

$$\Delta v_r = \frac{f_c}{2c \cdot T_{CIT}} \tag{6}$$

where T_{CIT} represents the CIT in seconds. The CIT is determined based on the radial velocity difference required for MSF recognition. The actual radial velocity difference between sub-targets is represented as:

$$\Delta v_r' = \frac{d \cdot R_0 \sin\theta_0 \cdot \omega}{\sqrt{\left(R_0\cos\theta_0 + v_{ship}T_{CIT}\right)^2 + \left(R_0\sin\theta_0\right)^2}} \tag{7}$$

where d is the distance between the adjacent sub-targets, v_{ship} is the sailing speed, and ω is the rotational angular velocity of the formation center relative to the radar. If $\Delta v_r < \Delta v_r'$ is met, the sub-targets of the formation can be recognized theoretically.

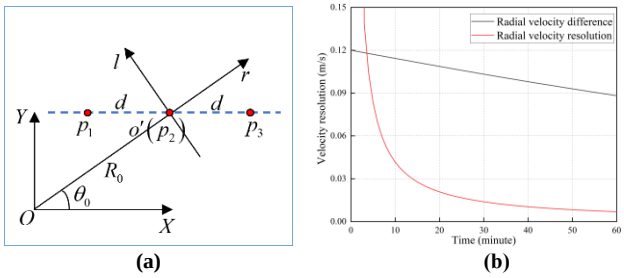

(a) (b)

Fig. 1 The single-column formation. (a) The geometric model of the single-column formation. (b) The variation of radial velocity resolution and radial velocity difference of sub-target with CIT.

Fig 1(a) shows the single-column formation geometric model, and Fig 1(b) shows the variation of radial velocity resolution and radial velocity difference of sub-target p_1 with CIT. For an ideal scenario, the provided radial velocity resolution is lower than the radial velocity difference when the CIT reaches 4 minutes, which can meet the requirements for MSF recognition. Due to the interference term $2f_c r_i / c$ in Eq. 4, the signal amplitude of the sub-target is to some extent affected by r_i . It is validated with experiments that the CIT is set to approximately 8 minutes, and the MSF recognition effect is perfect. Table 3 compares the required CIT for ideal and actual scenarios.

Table 3 CIT for single-column formation.

Parameter Name	Ideal scenario	Actual scenario
CIT	4 min	8 min
Radial velocity resolution	0.104 m/s	0.052 m/s
Radial velocity difference	0.118 m/s	0.115 m/s

Fig 2 shows the V-shaped formation and symmetrical formation geometric model. In Figure 2(a), $\beta_1 = 2\pi/3$, $\beta_2 = \pi/6$, d_1=3 km, d_2=2 km. In Figure 2(b), the sub-targets are symmetrically distributed with equal distances from the formation center. The angle between two sub-targets is

$2\pi/3$. As shown in Table 4, the optimal CIT for the V-shaped and symmetrical formation is determined through multiple simulation experiments. For the V-shaped formation, the required CIT increases due to the interference term. For the symmetrical formation, the velocity projections of p_1 and p_3 in the radial direction are consistent. A longer CIT is needed for recognition ideally. In practice, the radial range between p_1 and p_3 is different, exacerbating the differences in the echo amplitude from sub-targets. This to some extent shortens the CIT.

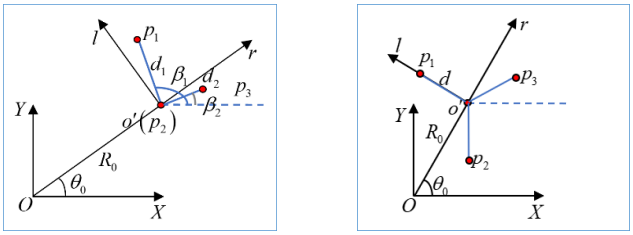

Fig. 2 The geometric model of two types of formation. (a) The V-shaped formation. (b) The symmetrical formation.

Table 4 CIT for V-shaped formation and symmetrical formation.

Formation	Parameter Name	Ideal scenario	Actual scenario
V-shaped formation	CIT	7 min	11 min
	Radial velocity resolution	0.060 m/s	0.038 m/s
	Radial velocity difference	0.065 m/s	0.062 m/s
Symmetrical formation	CIT	23 min	13 min
	Radial velocity resolution	0.018 m/s	0.032 m/s
	Radial velocity difference	0.020 m/s	0.012 m/s

3.2 Formation recognition experiment

The experiment process of MSF recognition is shown in Figure 3. Firstly, the actual RD background comes from the HFSWR station, which is located in Weihai, China. Three types of simulated formations, single-column, V-shaped, and symmetrical formations, are injected in the actual RD background. The radial range of the formation center to the radar is obtained with the CFAR method. Then, the 2D IFFT is performed on the RD images to obtain the echo signal in time domain. The imaging blurring, which is caused by the joint motion of sub-targets in long CIT, can be eliminated by motion compensation in time domain. Finally, the focused Doppler profile is obtained by FFT along the slow time. The sub-target quantity recognition of the formation through peak detection in the Doppler domain.

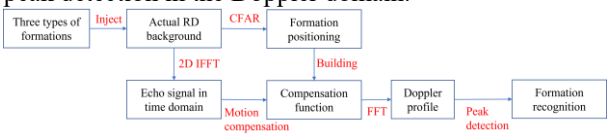

Fig. 3 The formation recognition process based on the actual RD background.

Figure 4 and Figure 5 compare the RD images and Doppler profile before and after motion compensation for single-column, V-shaped, and symmetrical formations. It can be seen that the compensated MSF signal undergoes spectral shift in the Doppler domain, and the Doppler spectrum is shifted to near 0 frequency. The values in the range domain have been added with R_0 compensation for correction for easier analysis. Before motion compensation, there is a significant broadening of the image in the Doppler direction. After motion compensation, Doppler broadening is eliminated, and the focused image shows the number of sub-targets in the formation. Different types of formations can be recognized with a sufficient amount of time.

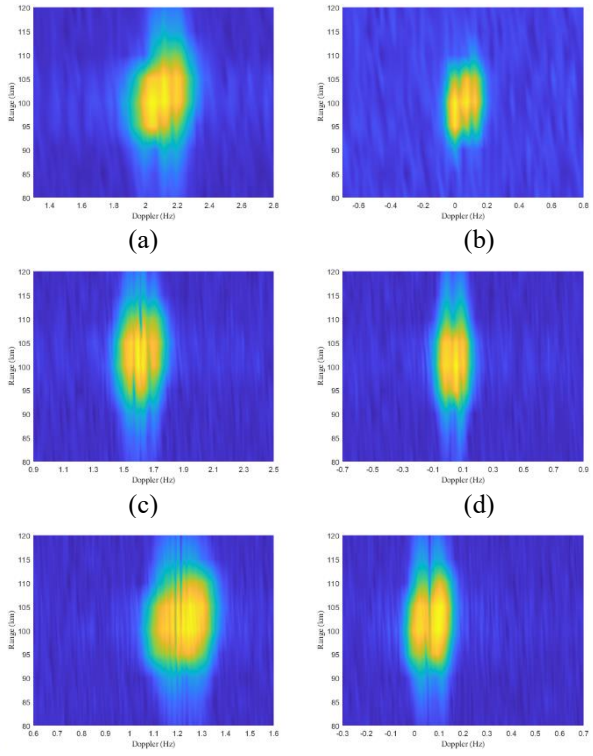

Fig. 4 The RD images. (a) In the situation of single-column formation without motion compensation. (b) In the situation of single-column formation with motion compensation. (c) In the situation of V-shaped formation without motion compensation. (d) In the situation of V-shaped formation with motion compensation. (e) In the situation of symmetrical formation without motion compensation. (f) In the situation of symmetrical formation with motion compensation.

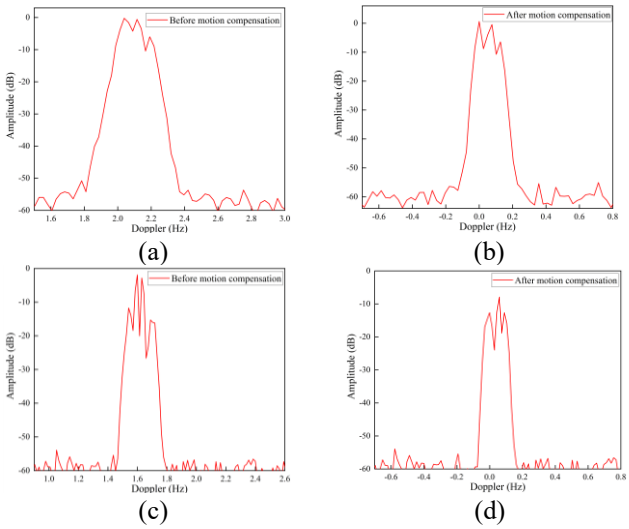

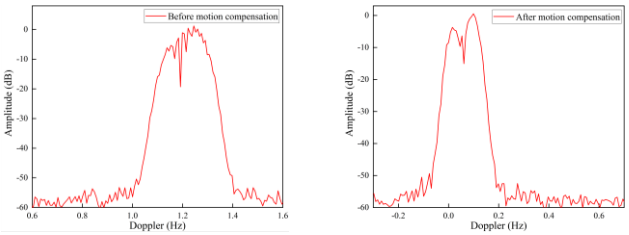

Fig. 5 The Doppler profile. (a) In the situation of single-column formation without motion compensation. (b) In the situation of single-column formation with motion compensation. (c) In the situation of V-shaped formation without motion compensation. (d) In the situation of V-shaped formation with motion compensation. (e) In the situation of symmetrical formation without motion compensation. (f) In the situation of symmetrical formation with motion compensation.

In practice, there are deviations in the position and velocity of the sub-targets, which may cause imaging bias. To test the robustness of the proposed MSF recognition method, the range parameter R_0 from MSF model is set to $\pm$ 2% float, the parameter v_{ship} is set to $\pm$ 10% float. There are 200 Monte Carlo samples for each formation. The variation of recognition accuracy with CIT is shown in Figure 6. For single-column and symmetrical formations, motion compensation can shorten the CIT required. For V-shaped formation, the improvement effect of motion compensation on MSF recognition is only demonstrated when the CIT is greater than 10 minutes.

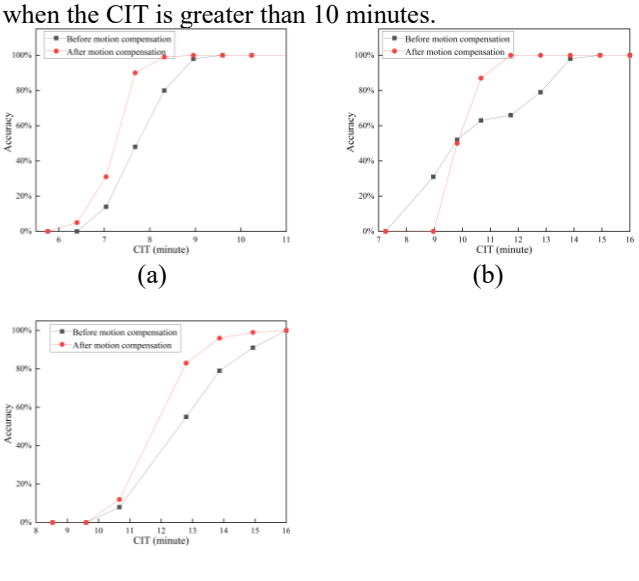

Fig. 6 The variation of recognition accuracy with CIT before and after motion compensation. (a) The single-column formation situation. (b) The V-shaped formation situation. (c) The symmetrical formation situation.

4. Conclusion

In this paper, the MSF signal model for high-frequency surface wave radar (HFSWR) is established, and the range-Doppler (RD) imaging method based on coherent accumulation and motion compensation is proposed. The peak detection is used to determine the sub-target number of the formation in the Doppler profile. We compare the theoretical coherent integration time (CIT) required for MSF recognition with the actual CIT using three types of formation models: single-column formation, V-shaped formation, and symmetrical formation. We design an experimental process based on the actual RD background, and verify the effectiveness of the proposed signal processing method without modifying the HFSWR system. Among them, the motion compensation method can effectively shorten the required CIT and improve the recognition accuracy. For the non-standard formation model, Monte Carlo experiments are conducted to verify the robustness of the recognition method proposed in this paper.

Acknowledgments

We are grateful to the editor and anonymous reviewers for their suggestions. This research and publication of the article were funded by the National Nature Science Foundation of China under Grant 62031015 and Mount Taishan Scholar Distinguished Expert Plan under Grant 20190957.

References

[1] H. Leong, and H. Wilson, “An estimation and verification of vessel radar cross sections for high-frequency surface-wave radar,” IEEE Antennas and Propagation Magazine, vol. 48, no. 2, pp. 11-16, 2006.

[2] D. Yao, X. Zhang, Q. Yang, and W. Deng, “A novel nonhomogeneous detector based on over-determined linear equations with single snapshot,” IEICE Transactions on Fundamentals of Electronics, Communications and Computer Sciences, vol. 102. no. 9, pp. 1312-1316, 2019.

[3] S. Grosdidier, and A. Baussard, “Ship detection based on morphological component analysis of high-frequency surface wave radar images,” Iet Radar Sonar and Navigation, vol. 6. no. 9, pp. 813-821, 2012.

[4] W. Sun, X. Li, Z. Pang, Y. Ji, Y. Dai, and W. Huang, “Track-to-Track Association Based on Maximum Likelihood Estimation for T/R-R Composite Compact HFSWR,” Ieee Transactions on Geoscience and Remote Sensing, vol. 61, pp. 5102012, 2023.

[5] Z. Yang, H. Zhou, Y. Tian, and J. Zhao, “Improved CFAR detection and direction finding on time–frequency plane with high-frequency radar,” IEEE Geoscience and Remote Sensing Letters, vol. 19, pp. 3505005, 2021.

[6] H. Rohling, “Radar CFAR thresholding in clutter and multiple target situations,” IEEE Transactions on Aerospace and Electronic Systems, vol. 19, no. 4, pp. 608-621, 1983.

[7] M. Ravan, and R.S. Adve, “Robust STAP for HFSWR in Dense Target Scenarios with Nonhomogeneous Clutter,” IEEE Radar Conference, 2012.

[8] X. Wang, Y. Li, and N. Zhang, “A robust constant false alarm rate detector based on the Bayesian estimator for the non-homogeneous Weibull Clutter in HFSWR,” Digital Signal Processing, vol. 106, no. 1, pp. 102831, 2020.

[9] F. Liang, Y. Zhou, H. Li, X. Feng, and J. Zhang, “Multi-Aircraft Formation Recognition Method of Over-the-Horizon Radar Based on Deep Transfer Learning,” IEEE Access, vol. 10, pp. 115411-115423, 2022.

[10] J. Wang, A. Liu, C. Yu, and Y. Ji, “Ship Formation Identification with Spatial Features and Deep Learning for HFSWR,” Remote Sensing, vol. 16, no. 3, pp. 577, 2024.

[11] J. Wang, A. Liu, and C. Yu, “Ship Formation Identification Method for HFSWR based on Deep Learning,” IEEE Radar Conference, 2024.